JACS
JOURNAL OF THE AMERICAN CHEMICAL SOCIETY

Article

pubs.acs.org/JACS

Reaction Mechanism in Crystalline Solids: Kinetics and Conformational Dynamics of the Norrish Type II Biradicals from α-Adamantyl-*p*-Methoxyacetophenone

Gregory Kuzmanich,[†] Cortnie S. Vogelsberg,[†] Emily F. Maverick,[†] José Carlos Netto-Ferreira,[‡] J. C. Scaiano,[‡] and Miguel A. Garcia-Garibay*[,†]

[†]Department of Chemistry and Biochemistry, University of California, Los Angeles, California 90095-1559, United States

[‡]Department of Chemistry and Centre for Catalysis Research and Innovation, University of Ottawa, Ottawa, Ontario, Canada K1N 6N5

Supporting Information

ABSTRACT: In an effort to determine the details of the solid-state reaction mechanism and diastereoselectivity in the Norrish type II and Yang cyclization of crystalline α-adamantyl-*p*-methoxyacetophenone, we determined its solid-state quantum yields and transient kinetics using nanocrystalline suspensions. The transient spectroscopy measurements were complemented with solid-state NMR spectroscopy spin−lattice relaxation experiments using isotopically labeled samples and with the analysis of variable-temperature anisotropic displacement parameters from single-crystal X-ray diffraction to determine the rate of interconversion of biradical conformers by rotation of the globular adamantyl group. Our experimental findings include a solid-state quantum yield for reaction that is 3 times greater than that in solution, a Norrish type II hydrogen-transfer reaction that is about 8 times faster in crystals than in solution, and a biradical decay that occurs on the same time scale as conformational exchange, which helps to explain the diastereoselectivity observed in the solid state.

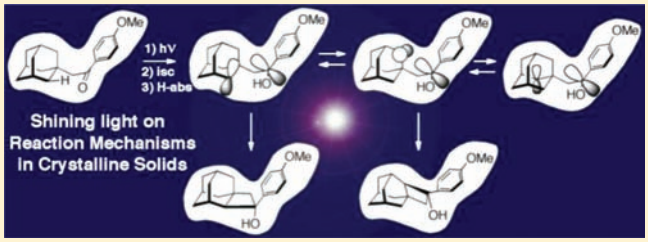

INTRODUCTION

Photochemical reactions in crystalline solids are not as common as those in the gas phase and in solution, but they tend to proceed with very high selectivities and specificities.[1] While it is widely appreciated that the nature of the products formed in crystals can be understood in terms of topochemical reaction pathways that are "least motion" in nature, detailed reaction mechanisms have been difficult to document. Most studies have been limited to product analysis and structure−reactivity correlations based on X-ray crystal structures of the reactant and the product,[2,3] which fail to disclose many crucial details of solid-state reaction mechanisms. To address these limitations, recent developments in the use of nanocrystalline suspensions for the spectroscopic characterization of electronic excited states and reactive intermediates now make it possible to document the kinetics of solid-state reactions in unprecedented detail.[4] Furthermore, if the dynamics of ground-state molecules within crystals are suspected to play a role in a solid-state reaction, they may be documented with several readily accessible solid-state NMR techniques and variable-temperature X-ray diffraction. Therefore, a wealth of information potentially available should make it possible to improve the understanding of reactions in the crystalline state.

In this paper, we report an example where these techniques are combined to gain unprecedented mechanistic detail of a solid-state photoreaction. Specifically, we report an investigation of the Norrish type II and Yang cyclization of α-adamantyl-*p*-methoxyacetophenone (**1**) (Scheme 1 and Figure 1).[5,6] This reaction sequence is one of the most widely studied and best understood photochemical transformations in solution and one of the most documented in the solid state.[7,8] For aryl alkyl ketones such as **1**, the Norrish type II reaction involves an intramolecular γ-hydrogen abstraction from the triplet excited state (^{3}**1** in Figure 1) to form a triplet 1,4-biradical (^{3}BR$_1$). The subsequent Yang cyclization involves the formation of a σ bond from the singlet-state biradical to yield cyclobutanols *cis*-**2** and *trans*-**3**.

Scheme 1

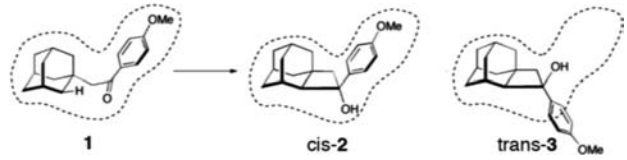

Studies by Scheffer and co-workers have shown that the reaction of α-adamantylacetophenones occurs efficiently in the crystalline state and that there is a good correlation between

Received: September 24, 2011
Published: December 7, 2011

   dx.doi.org/10.1021/ja2090004 | *J. Am. Chem.Soc.* 2012, 134, 1115−1123

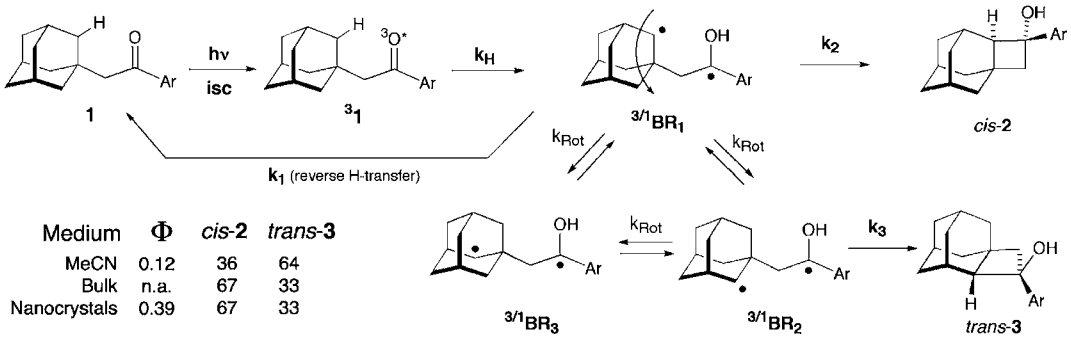

Figure 1. Photoexcitation of **1** results in cyclization products *cis*-**2** and *trans*-**3** in solution and in the solid state. The major diastereomer in solution is the less hindered *trans*-**3**. Photoreactions in the bulk solid and in nanocrystalline suspensions lead to the more hindered *cis*-**2** as the major diastereomer. The ratio of **2** to **3** in the solid is determined by the relative rates of adamantyl rotation from $^3BR_1$ and $^3BR_2$ followed by intersystem crossing and cyclization. Rotation to $^3BR_3$ results in a conformation that cannot undergo cyclization until a subsequent rotation to BR_1 or BR_2 occurs.

crystallographically determined ground-state conformations and reaction success.[7,8] Somewhat unexpectedly, however, ultraviolet irradiation of crystals of ketone **1** and other adamantylacetophenones was shown to give mixtures of *cis*-**2** and *trans*-**3**, with unpredictable product ratios. Specifically for **1**, the ratio of the diastereomeric photoproducts inverts when the reaction is performed in the solid state as compared to solution, yet product analysis and structure−reactivity correlations based on X-ray crystal structure data do not provide a full explanation. Therefore, the *p*-methoxy derivative **1** was identified as an interesting study subject on the basis of its spectroscopic and chemical properties, which include a relatively long-lived triplet state with mixed n,π^* and π,π^* character[9] that should make it possible to detect the triplet excited state and possibly the triplet biradical.

As indicated in Scheme 1, the formation of *cis*-**2** is a topochemically allowed, least-motion reaction that maintains good structural continuity between the shape of the starting ketone determined by single-crystal X-ray diffraction and the required shape of the *cis*-product. The relative orientations of the aromatic ring and the adamantyl group are retained in the reactant and the product, and it appears that the reaction should not be inhibited within the close-packed walls of the reaction cavity. In contrast, at a first approximation, the formation of *trans*-**3** may be considered unexpected as the aromatic anisole and the tricyclic adamantyl structures are on opposite sides in relation to the frame of reference provided by the reaction cavity of ketone **1**.

One of the structural features that unambiguously identifies the trajectories toward the two photoproducts is the absolute configuration of their quaternary cyclobutanol carbons. A subsequent study by Scheffer and Trotter with crystals of an enantiomerically pure adamantylacetophenone derivative showed that the two diastereomers possess the same absolute configurations at the newly formed carbinol carbon (differing by the configuration of the new adamantane chiral center, which also determines the *cis*/*trans* designation of the substituents on the cyclobutanol).[10] The implication of their study was that formation of *trans*-**3** does not involve rotation of the aromatic ring, which would expose different enantiotopic faces of the original carbonyl, but rather rotation of the more globular adamantyl group, as indicated in Scheme 2.

Knowing that the use of variable-temperature solid-state NMR spectroscopy and single-crystal X-ray diffraction analysis offers opportunities to characterize the rotational dynamics of

Scheme 2

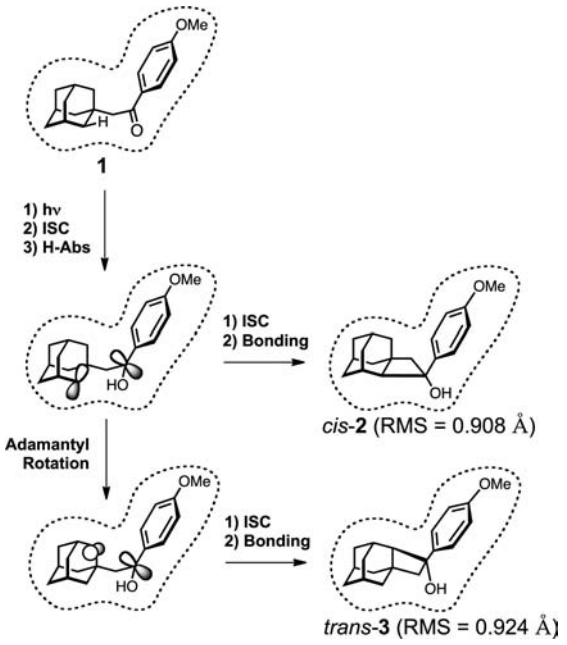

molecules in crystals, we set out to analyze the reaction mechanism of **1** through a combination of transient spectroscopic methods and solid-state dynamics characterization. As described in detail below, we discovered that the γ-hydrogen abstraction occurs with a time constant of ca. 10 ns from the triplet excited state to form the hydroxyadamantyl 1,4-biradical and that the latter decays with a time constant of 103 ns. We also discovered that the quantum yield of the solid-state reaction (Φ = 0.39) is ca. 3 times higher than that determined in acetonitrile solution (Φ = 0.12), in contrast to previous observations in the case of the di-π-methane reaction, which proceeds very sluggishly in the solid state.[11] Using variable-temperature spin−lattice relaxation experiments, it was established that rotation of the adamantyl group in the solid state at 300 K occurs by site exchange with a time constant of ca. 213 ns. This allows for a fraction of the biradicals to rotate within their lifetime, assuming that the rotation of the adamantyl group is similar in the ground-state ketone and the biradical states.

dx.doi.org/10.1021/ja2090004 | *J. Am. Chem.Soc.* 2012, 134, 1115−1123

RESULTS

Synthesis of α-Adamantyl-*p*-methoxyacetophenone (1). The synthesis of adamantylacetophenone **1** was accomplished as described in the literature by a Friedel–Crafts reaction of commercially available α-adamantylacetyl chloride and anisole. The structural identity of **1** was verified by ^{1}H and ^{13}C NMR, FT-IR, and melting point measurements that were consistent with those reported previously (Supporting Information).[6] Two isotopologues of **1** for solid-state NMR dynamics charaterization were synthesized in an analogous manner from commercially available methoxy-deuterated anisole (**1**-d_3) and perdeuterated anisole (**1**-d_7). Melting point and X-ray powder diffraction patterns of the isotopologues matched those of the natural-abundance sample, and the corresponding ^{1}H and ^{13}C solution NMR spectra contained the expected signals and peak splitting for close to 100% deuteration (Supporting Information).

Steady-State Photolysis in Solution, Bulk Powders, and Nanocrystalline Suspensions. Product analyses were carried out with dilute acetonitrile solutions or in crystalline solids using a Rayonet reactor with 312 nm lamps. As reported previously, adamantylacetophenone **1** reacts to give cyclobutanol diastereomers *cis*-**2** and *trans*-**3**, which differ by the relative orientation of the adamantyl moiety and aromatic ring with respect to the plane of the four-membered ring. Irradiation in acetonitrile preferentially led to the less hindered diastereomer, *trans*-**3**, in ca. 67% yield (Figure 1). Using valerophenone actinometry,[12] it was shown that the quantum yield of product formation at 312 nm is Φ_{Cyc} = 0.12 in argon-saturated acetonitrile. In agreement with previous reports,[6,13] irradiation of **1** as a dry polycrystalline powder switched the reaction selectivity to yield the more hindered diastereomer, *cis*-**2**, in 67% yield at low conversion values (Scheme 1). Photolysis experiments carried out at 312 nm with a nanocrystalline suspension in water[14,15] resulted in a diastereoselectivity of 67:33, which is identical to that obtained with bulk powders and single crystals. Notably, in contrast to the results obtained with dry solids, where the reaction diastereoselectivity decreases rapidly as a function of increasing conversion, the selectivity obtained with nanocrystals remained constant to conversion values as high as 80%. Nanocrystals of **1** were obtained by the reprecipitation method[16] with an average crystal size of ca. 200 nm as determined by scanning electron microscopy (SEM) and dynamic light scattering (DLS) measurements (Supporting Information). A comparison of the powder X-ray diffraction patterns of filtered nanoparticles and powdered bulk crystals confirmed that they correspond to the same polymorph as the single-crystal specimens used for single-crystal X-ray diffraction analysis (Supporting Information). Using dicumyl ketone (Φ_{-CO} = 0.18)[17] as a chemical actinometer at 312 nm, and with optically dense nanocrystalline suspensions in water, we determined the quantum yield of reaction of **1** in the solid state to be Φ_R = 0.39. Notably, this value is about 3 times greater than the value obtained for the same reaction in acetonitrile.

Transient Absorption Spectroscopy in Solution and in Nanocrystals. Given the high quantum yield of reaction in acetonitrile and in the nanocrystalline suspension, nanosecond transient absorption spectroscopy was explored on both phases. Excitation of adamantylacetophenone **1** at 355 nm (10 ns pulse) in a nitrogen-degassed acetonitrile solution led to one transient absorbing between 350 and 440 nm with λ_{max} = 385 nm (Figure 2, top). The entire band decays uniformly and monoexponentially with a lifetime of 80 ns. Previous work on hydrogen abstraction from *p*-alkoxyacetophenones has shown that hydrogen atom transfer occurs from the triplet state on nanosecond time scales,[18,19] and on the basis of the similarity of this transient with that previously reported for the triplet *p*-methoxyacetophenone chromophore,[20,21] we assign the band to the T_1 state of **1**. Further support for this assignment was obtained by quenching with oxygen. As the transient band decays uniformly, we conclude that the benzylic-type 1,4-biradical, expected to absorb at longer wavelengths,[19,22] must be too short-lived to accumulate and be observed.

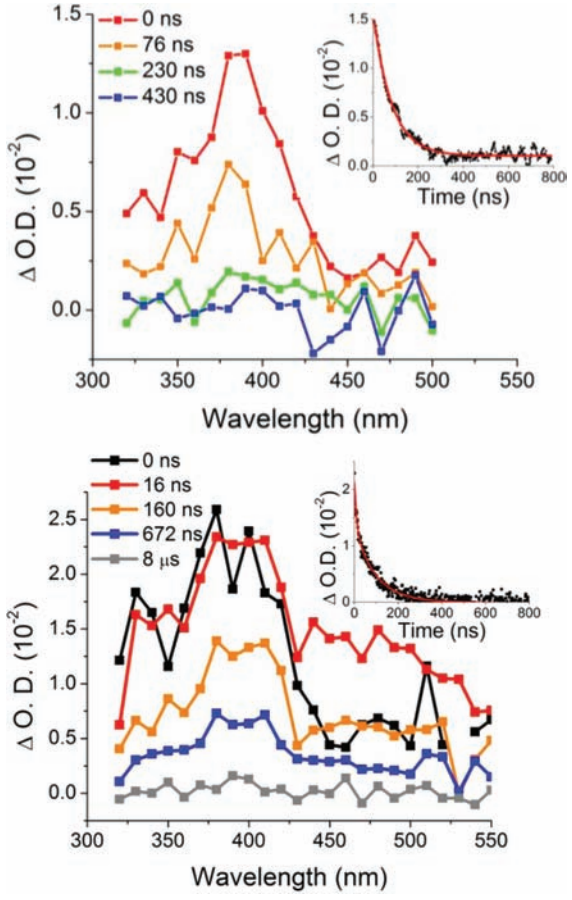

Figure 2. (Top) Transient absorption spectra of **1** in acetonitrile showing a λ_{max} = 385 nm assigned to the T_1 state of **1** with a monoexponential decay rate of 80 ns (inset). (Bottom) Transient absorption of **1** as a nanocrystalline suspension in water. The initial spectrum with a $\lambda_{max} \approx$ 380 nm is assigned to T_1 and the spectrum after 16 ns with absorbance at 400–550 nm to the triplet biradical. The transient could be fit with a biexponential function with lifetimes of 10 ns (T_1) and 103 ns (^{3}BR).

In contrast to the results obtained in solution, the excitation of **1** as a nanocrystalline suspension in water produces a broader band that expands from 320 to 450 nm with $\lambda_{max} \approx$ 390–400 nm (shown with a black line in Figure 2, bottom). After the initial formation of this transient, a broad shoulder between 450 and 550 nm develops within ca. 10 ns. After that, the entire spectrum decays uniformly from 320 to 550 nm. The decay of these transients could be fit to a biexponential function with lifetimes of 10 and 103 ns. The narrow spectrum formed immediately after the pulse (shown with a black line in the bottom frame of Figure 2) is an excellent match to the T_1 state of **1** in acetonitrile and is assigned to the T_1 state of **1** in the

dx.doi.org/10.1021/ja2090004 | J. Am. Chem.Soc. 2012, 134, 1115–1123

solid state with a lifetime τ_T = 10 ns. This transient has been documented in solution,[20a−c,23] in inclusion complexes,[20d] and absorbed in zeolite powders.[20e] The *p*-methoxy ketyl radical chromophore, responsible for the absorption spectrum of the 1,4-biradical, has also been documented.[23] As shown by the red line in the bottom frame of Figure 2, the spectrum consists of two bands with λ_{max} at 400 and 450 nm. Knowing that the quantum yield of reaction is high, we can assign the transient responsible for the longer lived component to the triplet biradical (^{3}BR).[23]

X-ray Diffraction Analysis. The single-crystal X-ray structure of adamantyl ketone **1** had been previously determined at ambient temperature by Scheffer et al. in the space group $P2_1/n$.[13] With the goal of exploring the rotational dynamics of the adamantyl group by analysis of the anisotropic displacement parameters, we redetermined the structure at 100, 200, and 300 K.[25] The structures obtained at these temperatures agreed with that reported previously, with a conformation that places the adamantyl group nearly orthogonal to the plane of the conjugated aromatic carbonyl (Figure 3) and a packing structure characterized by segregated

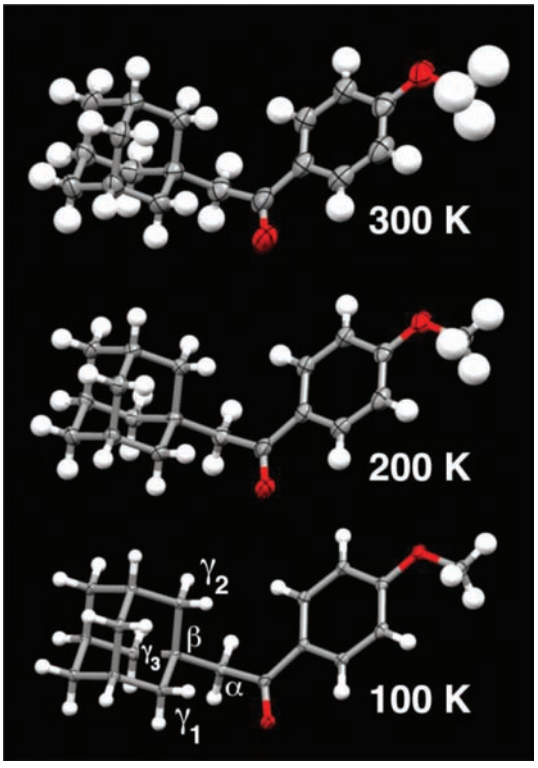

Figure 3. Molecular structure of **1** in the crystal at 100, 200, and 300 K. Thermal ellipsoids are shown at 50% probability. C atoms that are α, β, and γ to the carbonyl C are labeled in the 100 K structure. Distances at 100 K: carbonyl C···γ_1 = 3.015(1) Å, C···γ_2 = 3.228(1) Å, C···γ_3 = 3.877(1) Å (MercuryCSD[24]). Initial H abstraction occurs at γ_1 to form a radical center at that site. Ring closure may occur directly or after conformational equilibration by rotation of the adamantyl group (see the text).

layers of alternating aromatic moieties and adamantyl groups (Figure 4). As illustrated in Figure 3 (bottom structure), there are three symmetrically related γ-carbons in the adamantyl group, γ_1, γ_2, and γ_3, which could in principle act as hydrogen donors. However, only one of the hydrogens in γ_1 has the geometry required for excited-state transfer to the carbonyl

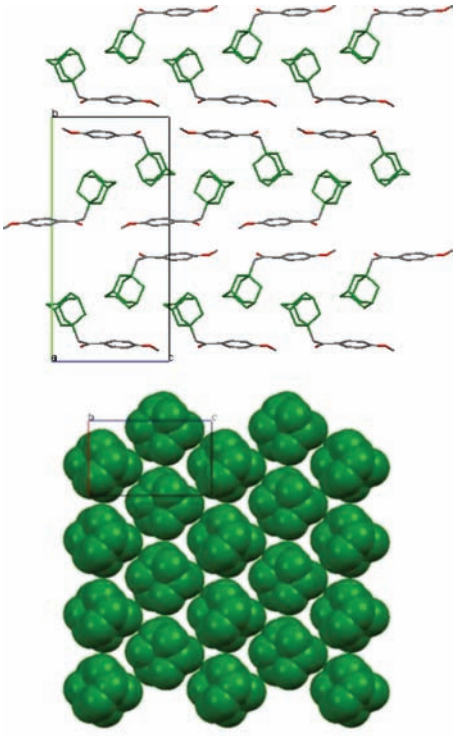

Figure 4. (Top) View of **1** along the *a* axis of the unit cell, showing the layered structure. Aromatic moieties are shown in gray and adamantyl moieties in green. (Bottom) View of the adamantyl layer along the *b* axis of the unit cell. The globular adamantyl moieties, shown here in space-filling mode, are hexagonally packed within layers. Hydrogens are omitted for clarity.

oxygen in the solid state to generate the hydroxy 1,4-biradical intermediate BR_1.[8] Knowing that rotation of the adamantyl groups in the solid state can be relatively fast, one can recognize that rotation of the adamantyl group about the $\alpha-\beta$ bond would result in the three conformationally distinct triplet biradicals shown in Figure 1: BR_1, BR_2, and BR_3. The three sites are related to the positions of the three γ-carbons and are related to each other by a 120° rotation of the adamantyl group about the α-methylene and adamantyl bridgehead β-carbon (Figure 3).

Reaction Cavity (Root-Mean-Square Difference) Analysis. It is generally acknowledged that formation of a given product in the solid state is more likely when its size and shape, and those of its corresponding transition state, are a good match to the size and shape of the reactant.[26,27] First suggested by Cohen, this concept is often shown as in Schemes 1 and 2 to illustrate what is known as the "reaction cavity". To determine the structural similarities between each of the two products and the starting reactant, one can determine the root-mean-square difference (rmsd) of their best overlap. Using the program PyMOL,[28] we set out to determine the rmsd of adamantylacetophenone **1** and model structures of the cyclization products *cis*-**2** and *trans*-**3**.[29] The ground-state conformation of **1** was taken directly from the X-ray structure. The structures of *cis*-**2** and *trans*-**3** were obtained by geometric optimizations (MM2) starting from initial modifications of the structure of **1** while keeping the *p*-methoxyacetophenone frozen. Rmsd values were obtained by comparing the best overlap between all non-hydrogen atoms in the starting material and the calculated product structures. As illustrated in Scheme 2, the results

dx.doi.org/10.1021/ja2090004 | J. Am. Chem.Soc. 2012, 134, 1115−1123

suggest that both products have an excellent structural overlap. Compounds *cis*-**2** and *trans*-**3** have rmsd values of 0.908 and 0.924 Å, respectively. We interpret these values as an indication that the formation of *trans*-**3** in crystals of **1** is as favorable as formation of *cis*-**2**, as long as the reaction mechanism involves the rotation of the adamantyl group to populate biradical conformers BR_2, presumably within the intersystem crossing limited lifetime of ca. 103 ns.[30] It should also be noted that BR_1 should have a high propensity to go back to the starting material, which has the perfect structural overlap with an rmsd = 0 Å.

Adamantyl Rotational Dynamics via Solid-State NMR ^{1}H Spin−Lattice Relaxation. It is well-known that globularly shaped bicyclic molecules tend to undergo rapid volume-conserving rotation in the solid state.[31,32] Supporting evidence for fast adamantyl rotation in the solid state was first obtained from the ^{13}C CP/MAS NMR spectrum, which displays rotationally averaged resonances for each of the three sets of crystallographically nonequivalent adamantyl carbons at positions γ, δ, and ε (designated with respect to the carbonyl group; please see the Supporting Information). To characterize the rotational dynamics of the adamantyl group of **1** in more detail, we decided to explore the use of ^{1}H NMR spin−lattice relaxation as a function of temperature, both in the laboratory (^{1}H T_1) and in the spin-locked rotating frames (^{1}H $T_1\rho$). These methods are based on the fact that the spin−lattice relaxation of nuclear spins in condensed phases may occur via stimulated transitions arising from dynamic processes within the lattice.[32] If a given conformational motion or group rotation modulates a magnetic interaction (e.g., dipolar coupling) and occurs at a rate that is near the Larmor (T_1) or spin-locking radio ($T_1\rho$) frequencies in an otherwise rigid lattice, the field that it generates may dominate the nuclear relaxation kinetics of the sample. If the process responsible for relaxation is thermally activated and follows an Arrhenius behavior with a correlation time τ_c (eq 1), the relaxation may be characterized as a function

$$\tau_c^{-1} = \tau_0^{-1} \exp(-E_a/RT) \quad (1)$$

of temperature to elucidate its characteristic activation energy (E_a) and pre-exponential factor (τ_0^{-1}, or A). The fastest relaxation (shortest time) will occur when the rate of motion matches either the Larmor frequency of the spins under observation in the corresponding magnetic field (T_1) or the applied spin-locking radio frequency field ($T_1\rho$). For solid samples with strong spin dipolar coupling and rapidly exchanging groups undergoing Brownian rotation with a time constant τ_c, the temperature dependence of the spin−lattice relaxation times at the Larmor frequency can be fit to the Kubo−Tomita relaxation expression[33] (eq 2). Similarly, relaxation in a spin-lock radio frequency field will provide information about dynamic processes described by eq 3

$$^1\mathrm{H}\ T_1^{-1} = C[\tau_c(1+\omega_0{}^2\tau_c{}^2)^{-1} + 4\tau_c(1+4\omega_0{}^2\tau_c{}^2)^{-1}] \quad (2)$$

$$^1\mathrm{H}\ T_1\rho^{-1} = C[(5/2)\tau_c(1+\omega_0{}^2\tau_c{}^2)^{-1} + \tau_c(1+4\omega_0{}^2\tau_c{}^2)^{-1} + (3/2)\tau_c(1+4\omega_1{}^2\tau_c{}^2)^{-1}] \quad (3)$$

at the corresponding lower frequency. The constant $C = (2/3)\gamma^2\mathbf{B}_{nuc}{}^2$ corresponds to dipolar interactions related to the relative positions of the nuclei that participate in the relaxation process. $\mathbf{B}_{nuc}$ is the static local effective dipolar field, γ and ω_0 are the gyromagnetic ratio and the angular Larmor frequency, respectively, of the observed nucleus in a magnetic field, and ω_1 is the angular frequency of the applied spin-locking field. The corresponding ^{1}H NMR frequencies in our experiments (in units of $\nu = \omega/2\pi$) are 300 MHz and 56 kHz for the laboratory and spin-locking fields, respectively.

As a starting point to characterize the rotational dynamics of the adamantyl group in crystals of **1**, experiments were carried out to probe a wide range of possible rotational frequencies. Both ^{1}H T_1 and ^{1}H $T_1\rho$ measurements were performed as a function of temperature from T = 235 K to T = 325 K on a static polycrystalline sample confirmed to be the same crystal phase via powder X-ray diffraction (PXRD) measurements. Unexpectedly, neither ^{1}H T_1 nor ^{1}H $T_1\rho$ relaxation kinetics could be fit to a single exponential function, preventing the unequivocal quantification of the adamantyl group rotational dynamics (Figures S10−S13, Supporting Information). Such nonexponential behavior is atypical in crystalline solids of a single phase, but it has been previously reported for methyl-containing structures and may be attributed to cross-correlation effects that retard the recovery of the magnetization.[34] As expected from a system without a common spin temperature or a single relaxation rate, the normalized ^{1}H wide-line spectra are kinetically heterogeneous (Figures S10b and S12b).

To eliminate the suspected effects of the methyl groups, a methyl-deuterated isotopologue was synthesized (**1**-d_3) and analyzed, knowing that deuterium cannot contribute to the proton spin−lattice relaxation. As expected, the relaxation for crystalline **1**-d_3 at all temperatures occurred without the presence of a significantly slower component. However, the kinetics of the magnetization recovery could not be satisfactorily fit to a single exponential function (Figures S14 and S15, Supporting Information). Finally, we speculated that a relatively efficient segregation of aromatic and adamantyl protons in the crystal packing (Figure 4) may prevent effective spin diffusion, which is required for the sample to reach a common spin temperature. To test this, we synthesized a second isotopologue with ^{2}H substitution at both methyl and phenylene groups (**1**-d_7). An added benefit of using this isotopologue is that the only protons in the sample belong to the highly mobile adamantyl group and to the rigid methylene α-carbon, so that any features observed in the relaxation data can be clearly assigned to the adamantyl. Satisfyingly, spin−lattice relaxation measurements on crystalline **1**-d_7 revealed a system with a common spin temperature, showing that isotopic substitution of the phenylene and methyl group protons resulted in the desired effect. Relaxation measurements of **1**-d_7 at 300 MHz and in a spin-lock field of 56 kHz from T = 235 K to T = 325 K were well behaved and characterized by a single exponential (Figures S18 and S20b, Supporting Information).

As illustrated in Figure 5, ^{1}H T_1 of **1**-d_7 at 300 MHz decreased as the temperature increased from 255 K, suggesting a dynamic process characterized by a rate approaching the Larmor frequency at higher temperatures (Figure 5, green rhombs). A relatively low melting point of 79−80 °C prevented the determination of the ^{1}H T_1 minimum necessary to fit the data to the full Kubo−Tomita eq 2. However, it can be shown that the low-temperature data have a slope equal to E_a/R, and a linear regression (R^2 = 0.9925, Figure 5) reveals an activation

dx.doi.org/10.1021/ja2090004 | J. Am. Chem.Soc. 2012, 134, 1115−1123

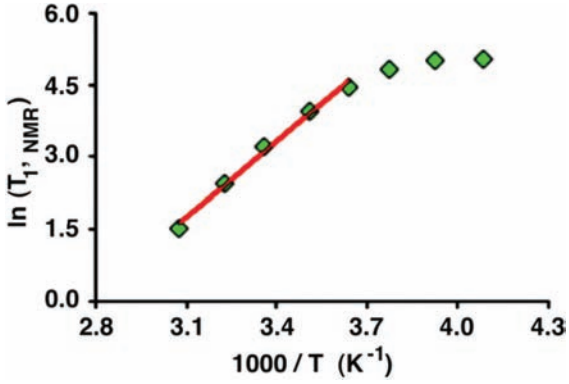

Figure 5. ln(^{1}H T_1) as a function of temperature for **1**-d_7 (green rhombs). The red line is a linear regression fit to the slope of the line, E_a/R. The activation energy E_a = 10.5 kcal mol^{-1}, and R^2 = 0.9925.

energy E_a = 10.5 kcal mol^{-1}.[35] This activation energy may seem rather high for a globular adamantyl group in the solid state, but is not unreasonable considering that it is engaged in five close contacts.

A series of ^{1}H $T_1\rho$ measurements at a spin-lock field of 56 kHz displayed behavior characteristic of a dynamic process undergoing rotation at a rate near the frequency of the applied spin-lock field at temperatures much lower than its melting point (Figure 6, yellow circles). A maximum at ca. 265 K

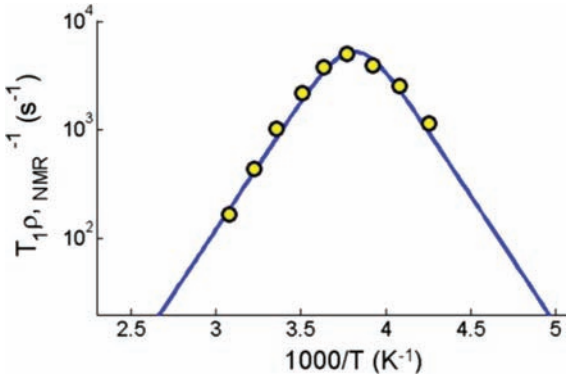

Figure 6. ^{1}H spin−lattice relaxation in the rotating frame (^{1}H $T_1\rho^{-1}$) measured on the **1**-d_7 isotopologue from T = 235 K to T = 325 K shows a temperature dependence, with a ^{1}H $T_1\rho^{-1}$ maximum at ca. 265 K (yellow circles) in a spin-lock field of 56 kHz. The heavy line corresponds to a Kubo−Tomita fit (eq 3) for the process assuming Arrhenius-type behavior (eq 1) with E_a = 10.8 kcal mol^{-1} and A = 3.92 × 10^{14} Hz.

indicates that the rotational process is in resonance with this field. A Kubo−Tomita fit (blue line, Figure 6) using eq 3 discloses an activation energy of 10.8 kcal mol^{-1}, in excellent agreement with that obtained from the ^{1}H T_1 experiments, and a constant C that is in excellent agreement with parameters from the crystal structure (Supporting Information). The fit also reveals a pre-exponential factor A = 3.92 × 10^{14} Hz (τ_0 = 2.55 × 10^{-15} s), which is rather large, but consistent with that observed for rotation of the parent adamantane molecule in its rigid-rotor plastic crystalline phase, where it undergoes rapid jumps between sites on its potential energy surface.[36] Importantly, from these activation parameters, we can calculate that the adamantyl group of **1** rotates at a time constant τ_c = 213 ns (k_{Rot} = 4.7 MHz) when T = 300 K.

Thermal Motion Analysis at Different Temperatures. The barrier to rotation of the adamantyl group in the crystalline state was also investigated by analysis of the anisotropic displacement parameters (ADPs) available from the single-crystal X-ray structures (Figure 3). The ADPs account for the space- and time-averaged positions of the atoms with contributions from static disorder and dynamic processes.[37] We have previously shown that ADP measurements can give rotational barriers that are comparable to the activation energies derived from variable-temperature solid-state NMR measurements.[38] The two analyses are complementary, in the sense that ADP analysis uses time-averaged electron density data from heavier atoms (C and O) as they oscillate at the bottom of the rotational potential wells, while NMR measurements involve changes in the magnetic interactions from the H atoms as a result of changes that occur over relatively short time scales as they move past the top of the potential. To analyze the ADPs in terms of a rotational energy profile for the adamantyl group, we used the thermal motion analysis program THMA14C written by Schomaker and Trueblood[39] and adapted in WinGX by Farrugia.[40]

As illustrated in Figure 3, variations in temperature from 100 to 200 and 300 K increase the size of the thermal ellipsoids, which are represented at the 50% probability level. In analogy to the solid-state NMR experiments, it was necessary to remove from the calculation groups that are undergoing faster motion in the crystal. For example, the displacement parameters of the methoxy group at 100 K are consistent with libration having an amplitude of about 30 deg^2, while the maximum amplitude of the adamantyl group plus the attached methylene carbon (analyzed as an isolated molecule) is about 5 deg^2. The adamantyl group at this temperature is held tightly in the crystal by short H···H and C···H contacts, but these contact distances are longer at 200 K and at 300 K. The libration amplitude about the axis defined by the $\alpha-\beta$ bond between the adamantyl quaternary carbon to the α-methylene carbon increases at the higher temperatures to about 12 and 21 deg^2, respectively. Notably, the angular displacement amplitude at the bottom of the well at 300 K is still relatively small, considering the relatively fast site exchange and lower barrier disclosed by the ^{1}H T_1 measurements. If one assumes a simple sinusoidal potential, the temperature dependence of the adamantyl group libration is consistent with a barrier height of ca. 20 kcal mol^{-1} for a 3-fold rotational potential and about 6 kcal mol^{-1} for a 6-fold potential. (Further details of this analysis are presented in the Supporting Information.) As illustrated in Figure 7, the larger the number of minima per rotational period for a given barrier height, the steeper the potential and the smaller the libration amplitude. Conversely, for a given libration amplitude, the smaller the number of minima, the higher the barrier.

The ADP-derived values for the barrier height (6 and 20 kcal mol^{-1}) are not consistent with the 10.5 and 10.8 kcal mol^{-1} barriers determined by ^{1}H T_1 and ^{1}H $T_1\rho$ NMR measurements, respectively. A possible explanation for this discrepancy was suggested by a force field analysis of the solid-state rotational potential using a cluster that considers only interactions with the nearest neighbors of a test adamantyl group in crystals of **1** (Figure 8 and Supporting Information). While the results are only qualitative as they pertain to the magnitude of the energetic barriers, they correctly reveal that, in addition to sites defined by the 3-fold symmetry of the adamantyl group, there are three higher energy sites displaced by ca. 60° from the first set. The shape of the rotational potential in Figure 8 accounts

dx.doi.org/10.1021/ja2090004 | J. Am. Chem.Soc. 2012, 134, 1115−1123

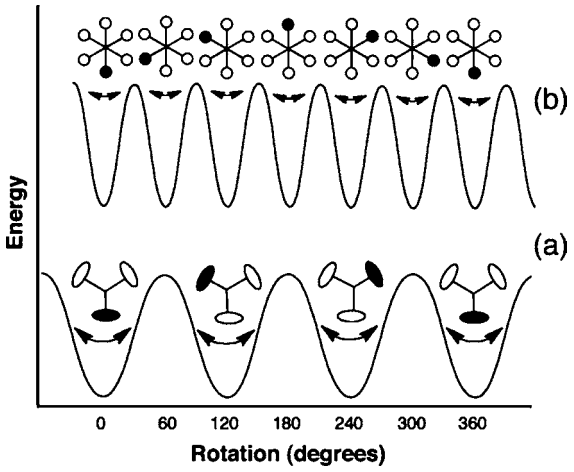

Figure 7. Representation of the relation between the ADP libration amplitudes, represented by the double arrows, and the symmetry order of a sinusoidal potential for 3-fold (a) and 6-fold (b) symmetries.

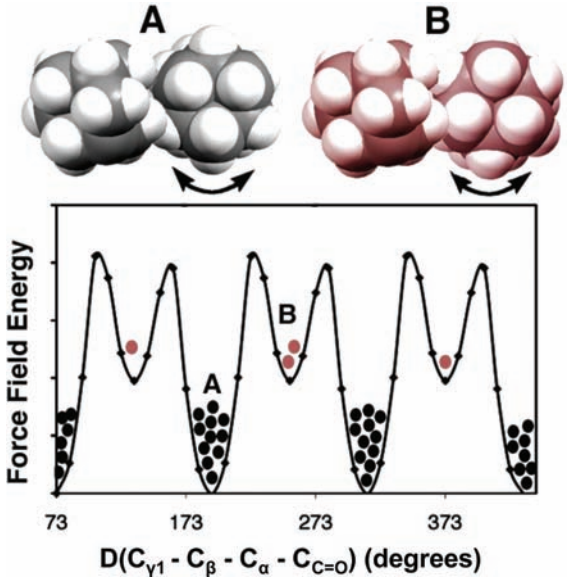

Figure 8. A force-field model for the rotation of the adamantyl group about the $\alpha-\beta$ bond of ketone **1** reveals two sets of energy minima (A, B) related by ca. 60°. Their relative energies differ by steric contacts with close neighbors, as illustrated by the top structures. Only the lowest energy rotamers (A) have a large enough population (dots) to be detected by X-ray diffraction. See Figure 3 for identification of the four atoms that define the dihedral angle *D* (the atoms are numbered C7−C6−C11−C12 in the X-ray structure).

for the small libration amplitude (or well width) of the adamantyl group estimated using ADPs (Supporting Information).[41] In other words, the rotational potential may be better represented by a combination of 6-fold and 3-fold functions, with wells of similar width but unequal depth, than by a single sinusoidal function.

■ DISCUSSION

The solution photochemistry of α-adamantylacetophenone derivatives was first reported by Lewis et al. in 1973.[42] It was shown that α-adamantylacetophenone in solution undergoes efficient γ-hydrogen abstraction to form a hydroxy 1,4-biradical, which subsequently undergoes a Yang cyclization to give two cyclobutanol products. As expected from a consideration of Bredt's rule, the adamantyl-centered 1,4-biradical cannot undergo cleavage of its 2−3 ($\alpha-\beta$) bond, as it avoids formation of the highly strained double bond in 1-adamantene. It was subsequently shown by Scheffer et al. that many adamantylacetophenone derivatives undergo the Yang cyclization in the solid state with diastereoselectivities that change in a somewhat unpredictable manner. Reactions in solution led to preferential formation of the less hindered cyclobutanol *trans*-**3**. In contrast, on the basis of their X-ray structures, reactions in crystals were expected to give exclusively the more hindered topochemical product *cis*-**2**,[6] yet it has been shown that the formation of *trans*-**3** is surprisingly common (Figure 1).

We report now that the use of 200 nm crystals suspended in water gives a reaction selectivity that is analogous to those obtained in single crystals and dry powders, but with the added advantage that the diastereoselectivity is maintained to much higher conversion values (i.e., 80%). A particularly interesting observation is that the quantum yield of reaction in the crystalline state ($\Phi_{R\text{-}Crys}$ = 0.39) is 3 times greater than that measured in solution ($\Phi_{R\text{-}Soln}$ = 0.12). As discussed below, we interpret this result as an indication that the triplet biradical can avoid a reverse hydrogen atom transfer back to the starting material by escape from its initial conformation (BR_1).

The kinetic scheme in Figure 1 incorporates the mechanistic elements considered for our analysis. It is well-known that the intersystem crossing of aromatic ketones gives quantum yields close to unity, which makes it reasonable to assume that the Norrish type II hydrogen-transfer reaction occurs along the triplet manifold. Note: The triplet lifetime of **1** measured by phosphorescence is ≥10 ms at 77 K, but it is not observable at 298 K. By contrast, the triplet lifetime of unreactive *p*-methoxyacetophenone is ≥10 ms at both 77 and 298 K. This and the transient kinetics results indicate that hydrogen abstraction quenches the T_1 of **1** with a rate that is greater by a factor of 10^6 at 298 K. This indicates that the assumption that $\Phi_{ISC} \approx \Phi_{H\text{-}Abs} \approx 1$ is valid. The fact that there are no transients after the triplet ketone in solution indicates that the subsequent biradical ^{3}BR does not accumulate. A modest quantum yield of reaction of 0.12 in solution indicates that the primary decay pathway for the triplet biradical involves fast intersystem crossing (Figure 1, $^3BR_1$ to $^1BR_1$) and reverse hydrogen atom transfer to the starting ketone (^{1}BR to **1**). A lifetime of 80 ns for ^{3}**1** suggests an upper limit for the lifetime of the hydroxy 1,4-biradical in acetonitrile solution.

As it pertains to the solid-state reaction, the rate of hydrogen atom transfer is about 8 times faster than in solution, with a time constant of 10 ns from ^{3}**1** to $^3BR_1$. However, in contrast to the short biradical lifetime inferred in solution, the lifetime of the triplet biradical is extended to ca. 113 ns in the solid state. Considering that the time constant for biradical isomerization by rotation of the adamantyl group is ca. 213 ns, if one assumes that rotations in the ground state and excited state are similar, it may be concluded that product formation and return to the starting ketone will depend on a complex interplay of conformational dynamics and product-forming rates. The interconversion of the three radical conformers ($^3BR_1$, $^3BR_2$, and $^3BR_3$) obtained by rotation of the adamantyl group (k_{Rot}) is illustrated in Figure 1, along with their overall reaction rates k_1, k_2, and k_3. It is well-known that the rates of reaction for 1,4-biradicals in solution are limited by conformationally determined intersystem crossing to the singlet state, with bond formation occurring very fast in the singlet manifold.[43] Given that there is a single, long-lived biradical transient, it is

dx.doi.org/10.1021/ja2090004 | J. Am. Chem.Soc. 2012, 134, 1115−1123

likely that the spin states of the three biradicals in crystals may be spin-state-equilibrated with rates of reaction from each biradical conformer limited by rigidity effects.

Elegant studies in solution have shown that it is possible to determine the absolute rate constants for reactions from rapidly equilibrating 1,4-biradicals by considering the Curtin–Hammett postulate.[44,45] However, with comparable equilibrium and reaction kinetics, biradicals from adamantylacetophenone **1** in the solid state depart substantially from those conditions.[46] Fortunately, Andraos has presented the complete and exact time-dependent kinetic analysis for a variety of kinetic schemes involving various scenarios, including the one suggested in Figure 1, with one reactive conformer initially formed ($^3BR_1$) that undergoes interconversion with one reactive ($^3BR_2$) conformer and one unreactive conformer ($^3BR_3$).[47] Integral to the solution of the corresponding overall rates is the need to know the relative quantum yields of product formation and the independent rates of conformational interconversion (k_{Rot}, or τ_c^{-1} in eq 1). The exact solution is given by the following equations:

$$\Phi_1/\Phi_3 = \Phi(k_1/k_3) \tag{4}$$

$$\Phi_2/\Phi_3 = \Phi(k_2/k_3) \tag{5}$$

$$\Phi = [([^3BR_1]_0 + [^3BR_2]_0)(3k_{Rot}^2) + (2k_{Rot}^2k_3)[^3BR_1]_0]/[([^3BR_1]_0 + [^3BR_2]_0)(3k_{Rot}^2) + (2k_{Rot}^2k_2)[^3BR_1]_0] \tag{6}$$

$$k_{BR} = k_1 + k_2 + k_3 \tag{7}$$

where Φ_1, Φ_2, and Φ_3 are the quantum yields for biradical return to **1**, formation of *cis*-**2**, and formation of *trans*-**3**, respectively. The initial concentrations of the triplet biradicals are $[^3BR_1]_0$, $[^3BR_2]_0$, and $[^3BR_3]_0$, and k_{BR} is the measured biradical lifetime. If one assumes that (a) ketone intersystem crossing and triplet hydrogen abstraction occur with unit efficiency, (b) hydrogen abstraction results only in the formation of $^3BR_1$, and (c) unbiased rotation occurs among conformers $^3BR_1$, $^3BR_2$, and $^3BR_3$, then it is possible to calculate the individual rates of cyclization to obtain *cis*-**2** and *trans*-**3**, as well as the rate of reverse hydrogen abstraction that yields **1**. Under these assumptions, this kinetic analysis yields $k_1 = 5.77 \times 10^6$ s^{-1}, $k_2 = 2.47 \times 10^6$ s^{-1}, and $k_3 = 1.46 \times 10^6$ s^{-1}. The corresponding lifetimes are $\tau_1 = 173$ ns, $\tau_2 = 405$ ns, and $\tau_3 = 685$ ns.

One of the most interesting aspects of the solid-state reaction is the enhanced stereospecificity and increased quantum yield as compared to those of the reaction in solution. The initial formation and preferential reactivity of BR_1 to yield *cis*-**2** as the major product is the normal expectation for reactions carried out in the solid state, as suggested by the good size and shape correspondence between the ground-state ketone conformer and the *cis*-product (illustrated in cartoon manner in Scheme 1). It is interesting that the formation of *trans*-**3** is made possible, and even favorable, by a change in conformation of the original 1,4-biradical. The relative magnitudes of the rates of cyclization to form *cis*-**2** and *trans*-**3** from BR_1 and BR_2, respectively, are in good qualitative agreement with the computed differences in molecular shape of the products and the starting material illustrated in Scheme 2 (rmsd = 0.908 and 0.924 Å for *cis*-**2** and *trans*-**3**, respectively). The rate constants for reaction from BR_1 to *cis*-**2** and from BR_2 to *trans*-**3** differ by less than a factor of 2 ($k_2 = 2.47 \times 10^6$ s^{-1} vs $k_3 = 1.46 \times 10^6$ s^{-1}), suggesting that formation of *cis*-**2** requires "less" structural reorganization and presumably causes less local stress in the crystal lattice.

Given the detailed kinetics discussed above, we find the enhanced quantum yield of reaction in the solid state remarkable, as the rate of reverse hydrogen transfer from BR_1 ($k_1 = 5.77 \times 10^6$ s^{-1}) is very similar to the rate of reaction to *cis*-**2** ($k_2 = 2.47 \times 10^6$ s^{-1}). While it would be reasonable to expect that reverse H atom transfer would be extremely favorable, as it involves no overall motion of the molecule before and after "reaction", our results indicate that the trajectory from BR_1 to the ground-state ketone must be less favorable than that from ^{3}**1** to BR_1. In fact, the geometric disposition of the transferring adamantyl C–H atom and the singly occupied n-orbital in the triplet ketone are very different from those of the O–H hydrogen and the adamantyl p-orbital in the 1,4-biradical.

CONCLUSIONS

We have characterized the dynamics and kinetics of a solid-state photochemical reaction with unprecedented detail. Nanocrystalline suspensions were used to determine the quantum yield of product formation and the lifetimes of excited-state intermediates in the Yang cyclization reaction of α-adamantyl-*p*-methoxyacetophenone (**1**). A combination of solid-state NMR spectroscopy and analysis of ADPs of crystalline **1** uncovered adamantyl group rotational dynamics, which may interconvert biradical conformers in the solid state at a rate similar to that of cyclization. The combined evidence suggests that cyclobutanol *cis*-**2** forms from the initially formed 1,4-biradical ($^3BR_1$) and that cyclobutanol *trans*-**3** from a conformer ($^3BR_2$) reached by rotation about the ketone α–β bond, explaining the diastereoselectivity observed in the solid state. We believe that the results of this study will provide a starting point to analyze the detailed mechanisms of analogous solid-state reactions. Studies addressing other alkoxy derivatives with different packing motifs and similar excited-state properties are now under way to obtain structure–activity correlations based on single-crystal X-ray structures, solid-state dynamics, and nanocrystalline transient kinetics.

ASSOCIATED CONTENT

Supporting Information

Synthetic procedures and spectral characterization of all compounds, solid-state NMR spectra for all isotopologues of **1**, details of the Kubo–Tomita fit, computational results, and photochemical procedures. This material is available free of charge via the Internet at http://pubs.acs.org.

AUTHOR INFORMATION

Corresponding Author

mgg@chem.ucla.edu

ACKNOWLEDGMENTS

We thank Matthew N. Gard for helping with the SEM microscopy images, Dr. Cecil Dybowski for loaning the Bruker ^{1}H solid-state NMR wide-line probe to the University of California, Los Angeles, and the National Science Foundation for funding. We are grateful to the National Science Foundation for support through Grants CHE-0844455 and DGE0114443 (IGERT MCTP) for a training fellowship to G.K. and C.S.V.

REFERENCES

(1) For leading references, see: (a) Shiraki, S.; Garcia-Garibay, M. A. In *Handbook of Synthetic Photochemistry*; Albini, A., Faginini, M., Eds.; Wiley-VCH: Weinheim, Germany, 2010; p 25. (b) Yang, C.; Xia, W. *Chem.—Asian J.* **2009**, *4*, 1774. (c) MacGillivray, L. R.; Papaefstathiou, G. S.; Friscic, T.; Hamilton, T. D.; Bucar, D.-K.; Chu, Q.; Varshney, D. B.; Georgiev, I. G. *Acc. Chem. Res.* **2008**, *41*, 280. (d) MacGillivray, L. R. *J. Org. Chem.* **2008**, *73*, 3311. (e) Mortko, C, J.; Garcia-Garibay, M. A. *Top. Stereochem.* **2006**, *25*, 205. (f) Toda, F. *Top. Curr. Chem.* **2005**, *254*, 1. (g) Sakamoto, M. *Mol. Supramol. Photochem.* **2004**, *11*, 415.

(2) (a) Scheffer, J. R.; Garcia-Garibay, M. A.; Nalamasu, O. *Org. Photochem.* **1987**, *8*, 249. (b) Toda, F. *Acc. Chem. Res.* **1995**, *28*, 480. (c) Gamlin, J. N.; Jones, R.; Leibovitch, M.; Patrick, B.; Scheffer, J. R.; Trotter, J. *Acc. Chem. Res.* **1996**, *29*, 203. (d) Ramamurthy, V.; Venkatesan, K. *Chem. Rev.* **1987**, *87*, 433.

(3) (a) Naumov, P.; Sakurai, K.; Tanaka, M.; Hara, H. *J. Phys. Chem. B* **2007**, *111*, 10373. (b) Natarajan, A.; Tsai, C. K.; Khan, S. I.; McCarren, P.; Houk, K. N.; Garcia-Garibay, M. A. *J. Am. Chem. Soc.* **2007**, *129*, 9846.

(4) (a) Lebedeva, N. V.; Tarasov, V. F.; Resendiz, M. J. E.; Garcia-Garibay, M.A. .; White, R. C.; Forbes, M. D. E. *J. Am. Chem. Soc.* **2010**, *132*, 82. (b) Simoncelli, S.; Kuzmanich, G.; Gard, M. N.; Garcia-Garibay, M. A. *J. Phys. Org. Chem.* **2010**, *23*, 376. (c) Chin, K. K.; Natarajan, A.; Campos, L. M.; Johansson, E.; Shepherd, H.; Garcia-Garibay, M. A. *Chem. Commun.* **2007**, *41*, 4266.

(5) Scheffer, J. R.; Scott, C. In *CRC Handbook of Organic Photochemistry and Photobiology*; Hospool, W., Lenci, F., Eds.; CRC Press: Boca Raton, FL, 2004; p 54-1.

(6) Evans, S.; Omkaram, N.; Scheffer, J. R.; Trotter, J. *Tetrahedron Lett.* **1985**, *26*, 5903.

(7) (a) Scheffer, J. R.; Trotter, J.; Omkaram, N.; Evans, S. V.; Ariel, S. *Mol. Cryst. Liq. Cryst.* **1986**, *134*, 169. (b) Fu, T. Y.; Scheffer, J. R.; Trotter, J.; Yang, J. *Acta Crystallogr., Sect. C* **1998**, *C54*, 491. (c) Jones, R.; Scheffer, J. R.; Trotter, J.; Yang, J. *Tetrahedron. Lett.* **1992**, *33*, 5481. (d) Evans, S. V.; Omkaram, N.; Scheffer, J. R.; Trotter, J. *Tetrahedron. Lett.* **1986**, *27*, 1419. (e) Natarajan, A.; Mague, J. T.; Ramamurthy, V. *Cryst. Growth Des.* **2005**, *5*, 2348. (f) Scheffer, J. R.; Scott, C. In *CRC Handbook of Organic Photochemistry and Photobiology*; Hospool, W., Lenci, F., Eds.; CRC Press: Boca Raton, FL, 2004; p 54-1

(8) Gudmundsdottir, A. D.; Lewis, T. J.; Randall, L. H.; Scheffer, J. R.; Rettig, S. J.; Trotter, J.; Wu, C.-H. *J. Am. Chem. Soc.* **1996**, *118*, 6167.

(9) (a) Coulson, D. R.; Yang, N. C. *J. Am. Chem. Soc.* **1959**, *81*, 5061. (b) Wagner, P. J.; Hammond, G. S. *J. Am. Chem. Soc.* **1965**, *87*, 4009. (c) Yang, N. C.; Elliot, S. P. *J. Am. Chem. Soc.* **1969**, *91*, 7550. (d) Yang, N. D.; Elliot, S. P.; Kim, B. *J. Am. Chem. Soc.* **1969**, *91*, 7551.

(10) Jones, R.; Scheffer, J. R.; Trotter, J.; Yang, J. *Acta Crystallogr., Sect. B* **1994**, *50*, 601.

(11) Zimmerman, H. E.; Zuraw, M. J. *J. Am. Chem. Soc.* **1989**, *111*, 7974.

(12) Murov, S. L.; Carmichael, I.; Hug, G. L. *Handbook of Photochemistry*, 2nd ed.; Marcel Dekker: New York, 1993.

(13) Evans, S. V.; Trotter, J. *Acta Crystallogr., Sect. B* **1989**, *B45*, 500.

(14) Resendiz, M. J. E.; Taing, J.; Garcia-Garibay, M. A. *Org. Lett.* **2007**, *9*, 4351.

(15) Kuzmanich, G.; Gard, M. N.; Garcia-Garibay, M. A. *J. Am. Chem. Soc.* **2009**, *131*, 11606.

(16) Kasai, H.; Nalwa, H. S.; Oikawa, H.; Okada, S.; Matsuda, H.; Minami, N.; Kakuta, A.; Ono, K.; Mukoh, A.; Nakanishi, H. *Jpn. J. Appl. Phys.* **1992**, *31*, 1132.

(17) Veerman, M.; Resendiz, M. J. E.; Garcia-Garibay, M. A. *Org. Lett.* **2006**, *8*, 2615.

(18) Encina, M. V.; Lissi, E. A.; Lemp, E.; Zanocco, A.; Scaiano, J. C. *J. Am. Chem. Soc.* **1983**, *105*, 1856.

(19) For leading references on the kinetics of Norrish type II biradicals, please see: (a) Scaiano, J. C. *Acc. Chem. Res.* **1982**, *15*, 252. (b) Scaiano, J. C.; Lissi, E. A.; Encina, M. V. *Rev. Chem. Intermed.* **1978**, *2*, 139.

(20) (a) Lutz, H.; Breheret, E.; Lindqvist, L. *J. Phys. Chem.* **1973**, *77*, 1758. (b) Samanta, S.; Mishra, B. K.; Pace, T. C. S.; Sathyamurthy, N.; Bohne, C.; Moorthy, J. N. *J. Org. Chem.* **2006**, *71*, 4453. (c) Wismontski-Knittel, T.; Kilp, T. *J. Phys. Chem.* **1984**, *88*, 110. (d) Netto-Ferreira, J. C.; Scaiano, J. C. *J. Photochem. Photobiol.* **1988**, *45*, 109. (e) Wilkinson, F.; Willsher, C. J.; Casal, H. L.; Johnston, L. J.; Scaiano, J. C. *Can. J. Chem.* **1986**, *64*, 539.

(21) Carmichael, I.; Helman, W. P.; Hug, G. L. *J. Phys. Chem. Ref. Data* **1987**, *16*, 239.

(22) Johnston, L. J.; Scaiano, J. C. *Chem. Rev.* **1989**, *89*, 521.

(23) Fabbri, C.; Bietti, M.; Lanzalunga, O. *J. Org. Chem.* **2005**, *70*, 2720.

(24) Macrae, C. F.; Bruno, I. J.; Chisholm, J. A.; Edgington, P. R.; McCabe, P.; Pidcock, E.; Rodriguez-Monge, L.; Taylor, R.; van de Streek, J.; Wood, P. A. *J. Appl. Crystallogr.* **2008**, *41*, 466.

(25) The original crystal structure was published in ref 13. The supplementary crystallographic data for this paper, files CCDC 834759 to CCDC 834761, can be obtained free of charge from The Cambridge Crystallographic Data Centre via www.ccdc.cam.ac.uk/data_request/cif.

(26) Cohen, M. D. *Angew. Chem., Int. Ed Engl.* **1975**, *14*, 386.

(27) Example of site-dependentselectivities: Cheung, E.; Netherton, M. R.; Scheffer, J. R.; Trotter, J. *Org. Lett.* **2000**, *2*, 77.

(28) *The PyMOL Molecular Graphics System*, version 1.2r3pre; Schrödinger: New York.

(29) For refences on solid-statereactivity calculations similar to those used here, see: Angermund, K.; Klopp, I.; Krüger, C.; Nolte, M. *Angew. Chem., Int. Ed. Engl.* **1991**, *30*, 1354.

(30) Scaiano, J. C. *Acc. Chem. Res.* **1982**, *15*, 252.

(31) Parsonage, N. G.; Staveley, L. A. K. In *Disorder in Crystals*; Rowlinson, J. S., Baldwin, J. E., Eds.; Clarendon Press: Oxford, U.K., 1978.

(32) Fyfe, C. A. *Solid-State NMR for Chemists*; CFC Press: Guelph, Ontario, Canada, 1983.

(33) (a) Kubo, R.; Tomita, K. *Phys. Soc. Jpn.* **1954**, *9*, 888. (b) Redfield, A. G. *Adv. Magn. Reson.* **1965**, *1*, 1.

(34) (a) Cutnell, J. D.; Venable, W. *J. Chem. Phys.* **1974**, *60*, 3795. (b) Emid, S.; Wind, R. A. *Chem. Phys. Lett.* **1974**, *27*, 312. (c) Mehring, M.; Raber, H. *J. Chem. Phys.* **1973**, *59*, 1116. (d) Al-Haliaq, H. A.; Beckmann, P. A. *J. Chem. Soc., Faraday Trans.* **1993**, *89*, 3801.

(35) By considering therelaxation behavior in the limit of slow motion at low temperature,when $\omega_0^2\tau_c^2 \gg 1$, eq 2 can be simplified to ^{1}H $T_1^{-1} \approx (\omega_0^2\tau_c)^{-1}$. Also see: Taylor, R. E.; Bacher, A. D.; Dybowski, C. *J. Mol. Struct.* **2007**, *846*, 147.

(36) Johnson, R. D.; Yannoni, C. S.; Dorn, H. C.; Salem, J. R.; Bethune, D. S. *Science* **1992**, *255*, 1235.

(37) Wilson, C. C. *Crystallogr. Rev.* **2009**, *15*, 3.

(38) Khuong, T.-A. V.; Dang, H.; Jarowski, P. D.; Maverick, E.; Garcia-Garibay, M. A. *J. Am. Chem. Soc.* **2007**, *129*, 839.

(39) (a) Dunitz, J. D.; Schomaker, V.; Trueblood, K. N. *J. Phys. Chem.* **1988**, *92*, 856. (b) Schomaker, V.; Trueblood, K. N. *Acta Crystallogr., Sect. B* **1998**, *B54*, 507.

(40) Farrugia, L. J. *J. Appl. Crystallogr.* **1999**, *32*, 837.

(41) Maverick, E.; Mirsky, K.; Knobler, C. B.; Trueblood, K. N.; Barclay, L. R. B. *Acta Crystallogr., Sect. B* **1991**, *B47*, 272.

(42) (a) Lewis, F. D.; Johnson, R. W.; Johnson, D. E. *J. Am. Chem. Soc.* **1974**, *96*, 6090. (b) Lewis, F. D.; Johnson, R. W.; Kory, D. R. *J. Am. Chem. Soc.* **1974**, *96*, 6100. (c) Lewis, F. D.; Johnson, R. W.; Kory, D. R. *J. Am. Chem. Soc.* **1973**, *95*, 6470.

(43) Scaiano, J. C. *Tetrahedron* **1982**, *38*, 819.

(44) (a) Moorthy, J. N.; Koner, A. L.; Samanta, S.; Singhal, N.; Nau, W. M.; Weiss, R. G. *Chem.—Eur. J.* **2006**, *12*, 8744. (b) Singhal, N.; Koner, A. L.; Mal, P.; Venugopalan, P.; Nau, W. N.; Moorthy, J. N. *J. Am. Chem. Soc.* **2005**, *127*, 14375.

(45) Abe, M.; Kawakami, T.; Ohata, S.; Nozaki, K.; Nojima, M. *J. Am. Chem. Soc.* **2004**, *126*, 2838.

(46) Seeman, J. I. *Chem. Rev.* **1983**, *83*, 83.

(47) Andraos, J. *J. Phys. Chem. A* **2003**, *107*, 2374.